Journal of The Electrochemical Society, **154** (6) H512-H516 (2007)
0013-4651/2007/154(6)/H512/5/$20.00 © The Electrochemical Society

Improving Electrical Characteristics of $Ta/Ta_2O_5/Ta$ Capacitors Using Low-Temperature Inductively Coupled N_2O Plasma Annealing

Kou-Chiang Tsai,[a,b] Wen-Fa Wu,[a,z] Chuen-Guang Chao,[b] and Chi-Chang Wu[a,c]

[a]*National Nano Device Laboratories, Hsinchu, Taiwan*
[b]*Department of Materials Science and Engineering, and* [c]*Institute of Nanotechnology, National Chiao Tung University, Hsinchu, Taiwan*

The electrical characteristics of $Ta/Ta_2O_5/Ta$ capacitors are improved by treatments with inductively coupled N_2O plasma. A low-temperature (250°C) and short (5 min) process was used to reduce the leakage current and improve the reliability. A low leakage current density (4.0×10^{-10} A/cm^2 under 1 MV/cm), high breakdown field (4.2 MV/cm at 10^{-6} A/cm^2), and lifetime of over 10 years at 1.61 MV/cm is obtained for the $Ta/Ta_2O_5/Ta$ capacitor with the inductively coupled N_2O plasma treatment. The conduction mechanism of the leakage current in the $Ta/Ta_2O_5/Ta$ capacitor is discussed using current-voltage analyses and shows that the leakage current of the $Ta/Ta_2O_5/Ta$ capacitor is dominated by Schottky emission. N_2O plasma treatment can effectively reduce oxygen vacancies and the surface roughness of the Ta_2O_5 film, inhibiting the conduction of the leakage current.
 [DOI: 10.1149/1.2719624]

Manuscript submitted January 27, 2006; revised manuscript received January 26, 2007. Available electronically April 11, 2007.

There is an increased demand for high-performance capacitors for use as components of systems on chips (SoCs), which are essential in realizing rf and mixed-signal integrated circuit (IC) applications. Greater densities of the capacitors allow chips to be shrunk. Tantalum pentoxide (Ta_2O_5) has a higher dielectric constant (20–25), lower leakage current, greater breakdown strength, and lower loss tangent than other dielectrics.[1-3] However, the as-deposited Ta_2O_5 films have a large leakage current and poor dielectric breakdown. Several postannealing treatments have been suggested to improve the leakage currents of Ta_2O_5 films.[4] Therefore, annealing is required to improve the electrical characteristics of Ta_2O_5. Conventional furnace annealing usually maintains samples at high temperatures for a long time, and so it is inappropriate for IC technology.

Tantalum (Ta) is cheaper than precious metals such as platinum (Pt), palladium (Pd), and their alloys that are responsible for a large part of the production cost of the capacitors. It is therefore a strong candidate to replace precious metal electrodes for ferroelectric and complex oxide thin-film-based devices. Additionally, it acts as an effective diffusion barrier at the connection between metals.[5,6] In this paper, Ta was used as the electrode material for reactively sputtered Ta_2O_5 metal/insulator/metal (MIM) capacitors, and effects of the Ta electrode on the electrical and dielectric properties of Ta_2O_5 MIM capacitors were investigated.

One important mechanism of the leakage current is related to grain boundaries for Ta_2O_5 MIM capacitors. Although high-temperature annealing causes the as-deposited amorphous Ta_2O_5 film to crystallize into a polycrystalline film, it nevertheless generates leakage currents because of the grain boundaries. Previous studies have established that a polycrystalline Ta_2O_5 film that has been annealed at high temperatures has a larger leakage current than an amorphous Ta_2O_5 film.[4,7] However, problems associated with post-deposition annealing at a low annealing temperature for a short duration is unfavorable for the suppression in the leakage current,[8] as the oxidizing gases cannot be easily decomposed into oxygen atoms at low temperatures. This investigation introduces the advantages of post-treatment using an inductively coupled plasma (ICP) system. Previous studies have revealed the use of an ICP system to deposit a dense dielectric film at low temperatures, typically as low as room temperature, with a very low chamber pressure in the 1–10 mTorr range.[9-11] ICP treatment was expected to improve the electrical characteristics of Ta_2O_5 and ensure the reliability of the devices.

[z] E-mail: wfwu@mail.ndl.org.tw

Experimental

Test capacitors with an MIM structure were fabricated on SiO_2 (200 nm)/Si substrates. The Ta bottom electrodes with a thickness of 200 nm were deposited onto SiO_2/Si substrates by dc-magnetron sputtering using a highly pure tantalum target. After electrode deposition, 50 nm thick Ta_2O_5 thin films were deposited by relative sputtering. The sputtering chamber was evacuated to a base pressure of 1×10^{-7} Torr. The films were prepared at a power of 100 W and a constant pressure of 3.5 mTorr. As-deposited Ta_2O_5 films were subjected to various post-treatments to evaluate their effects. These were (*i*) N_2O plasma annealing at 250°C for 5 min in a plasma-enhanced chemical vapor deposition (PECVD) system (PE-N_2O), (*ii*) inductively coupled N_2O plasma at 250°C for 5 min in a high-density plasma CVD system (ICP-N_2O), (*iii*) annealing in a quartz tube furnace in O_2 ambient at 400°C for 30 min (F-O_2), and (*iv*) no annealing treatment (reference). Conventional plasma was generated using an rf (13.56 MHz) power supply connected to a showerhead plate with a power of 300 W and a N_2O flow rate of 200 sccm in a PECVD system. In the ICP system, an rf power source (13.56 MHz) is connected to the copper coil outside the ceramic plate of the upper chamber. The N_2O flow rate was 200 sccm, the ICP power was 300 W, and the process pressure was 5 mTorr. 200 nm thick Ta films were deposited by sputtering and patterned using shadow masks to form top electrodes after post-treatments of Ta_2O_5 films.

The thickness of the resulting Ta_2O_5 films was measured by scanning electron microscopy (SEM, JEOL JSM-6500F), which was also utilized to obtain the surface morphologies of the samples before and after annealing treatments. The surface roughness was elucidated by atomic force microscopy (AFM, Digital Instruments Nano-Scope III). Secondary ion mass spectrometry (SIMS, CAMECA IMS-5F) was employed to measure the relative atomic concentration and thus verify the variation in the composition. The electrical characteristics of the Ta_2O_5 MIM capacitors vs electric field and time were determined. During the electrical measurements, the top electrode was biased while the bottom electrode was grounded. The time-dependent dielectric breakdown (TDDB) properties were obtained under constant voltage stress using a Hewlett-Packard (HP) 4156B semiconductor parameter analyzer.

Results and Discussion

Figure 1 presents the leakage current densities of the reference, F-O_2, PE-N_2O, and ICP-N_2O samples as a function of electric field up to ±4.5 MV/cm. Asymmetric curves are observed for current density vs electric field (*J-E*) characteristics. After post-treatments, the leakage current is more decreased at a negative bias than at a positive bias. The leakage current at negative bias is influenced pri-

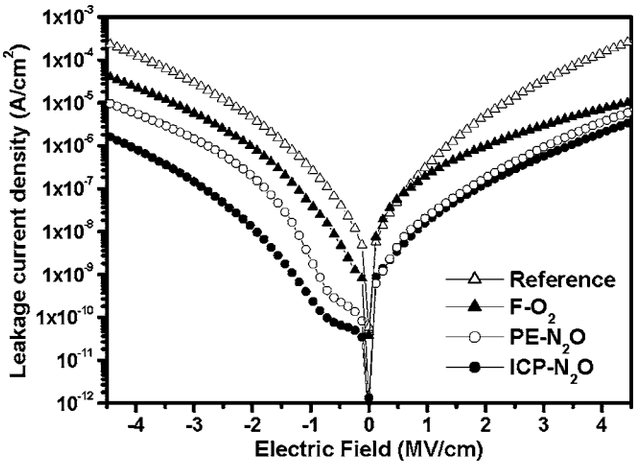

Figure 1. Leakage current densities of the Ta/Ta_2O_5/Ta capacitors before and after various post-treatments.

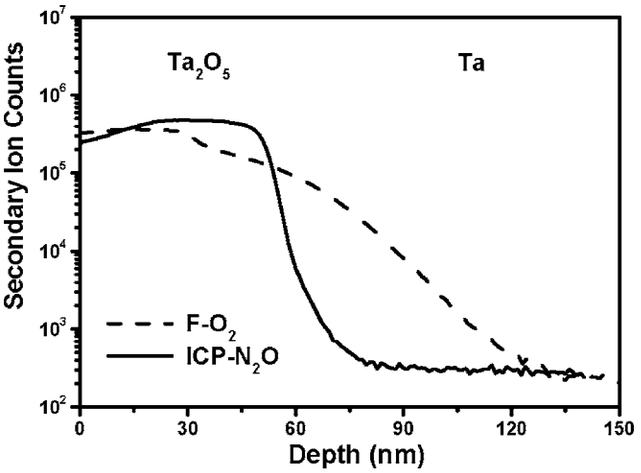

Figure 2. SIMS depth profiles of oxygen elements in Ta/Ta_2O_5/Ta capacitors after furnace annealing at 400°C for 30 min and ICP treatment at 250°C for 5 min.

marily by the interface of the Ta_2O_5 and Ta top electrode. The lowest leakage current densities were measured on the ICP-N_2O sample, yielding a value of 4.0×10^{-10} A/cm^2 at an electric field of −1 MV/cm, which is less than 3.8×10^{-9} A/cm^2 for the PE-N_2O sample, 3.8×10^{-7} A/cm^2 for the reference, and 5.7×10^{-8} A/cm^2 for the F-O_2 sample. Also, the leakage current density of the ICP-N_2O sample was lower than that in Ref. 12 at an electric field of 1 MV/cm. After the Ta_2O_5 films were deposited, the oxygen escaped and oxygen vacancies were formed, according to

$$O_o \leftrightarrow V_o'' + 2e^- + \frac{1}{2} O_2 \quad [1]$$

where O_o, V_o'', and e^- represent the oxygen ion in its normal state, an oxygen vacancy, and an electron, respectively. A high concentration of oxygen vacancies caused electrons to be generated and a large leakage current to flow. Treatment with oxygen-containing plasma yielded active oxygen atoms and reduced oxygen vacancies and ultimately improved the quality of Ta_2O_5 films.

Figure 1 indicates that the ICP-N_2O and PE-N_2O samples have better electrical characteristics than the F-O_2 sample. Many studies presented similar results and have established that the nitridation and oxidation are controlled by the mobility of nitrogen- and oxygen-based adatoms during the N_2O plasma treatment.[13-16] N_2O is a stronger oxidizing agent than O_2 because free O atoms are more easily produced according to the reaction[16,17]

$$O_2 \rightarrow 2\ O \quad [2]$$

$$e^- + N_2O \rightarrow NO + N + e^- \quad [3]$$

$$N + NO \rightarrow N_2 + O \quad [4]$$

The activation energy in Eq. 2 is 5.12 eV, whereas that in Eq. 3 and 4 is 2.51 eV. This result can be easily explained by the fact that less energy is required to break the N–O bond in a N_2O molecule than the O═O bond in an O_2 molecule. The excited oxygen atoms diffused rapidly into the Ta_2O_5 films and reduced the degree of imperfection and the concentration of oxygen vacancy. In addition, atomic N and surface-generated ions (NO) have been implicated in the nitridation process.

Figure 2 illustrates the SIMS depth profiles of the O elements in the F-O_2 and ICP-N_2O samples. The apparent oxygen diffusion found in the F-O_2 sample is because the oxygen atoms diffuse along the grain boundaries of the Ta crystal and react with the Ta bottom electrode layer during annealing. Nevertheless, almost no indication exists that oxygen atoms diffuse into the Ta bottom electrode layer in the ICP-N_2O sample due to low-temperature plasma treatment.

The leakage current density in the ICP-N_2O sample is much lower than that in the PE-N_2O sample at a negative bias, as displayed in Fig. 1. The influence of N_2O plasma on the Ta_2O_5 layer increases the concentration of oxygen atoms (or reduces the number of oxygen vacancies) in the Ta_2O_5 film. A PECVD system cannot generate high-density plasma. In fact, generating plasma even in a magnetic field at a chamber pressure of only a few mTorr is very difficult.[18] In an ICP system, a flowing rf current in the coils easily generates a changing magnetic field, which in turn induces a changing electric field through inductive coupling. Therefore, the inductively coupled electric field accelerates electrons at low pressure. The electronic mean free path may be shorter than the gap between the electrodes, so enough ionizing collisions occur. Hence, inductively coupled plasma reactors produce a high electron temperature that efficiently dissociates the N_2O gas under pressure and causes more O radicals and ions to be present. Previous studies demonstrated that the oxidant produced under high-density plasma discharge is more reactive than the primary reactant used in plasma O_2 annealing.[19] Accordingly, the high concentration of oxidants may explain why the leakage current density in the ICP-N_2O sample is lower than that in the PE-N_2O sample. Another reason may be the resulting roughness of the Ta_2O_5 layer. The Ta_2O_5 surfaces of the F-O_2 and PE-N_2O samples are clearly rougher than that of the ICP-N_2O sample, as displayed in Fig. 3. It is believed that the reactions or bombardments of energetic radicals and ions would occur during plasma treatment. They could sputter the films and make them smooth. The roughness effect can be interpreted as an image force that reduces the barrier height.[20,21] Table I summaries the electrical properties of Ta/Ta_2O_5/Ta capacitors with various post-treatments. The breakdown field is defined as the electric field when leakage current density exceeds 10^{-6} A/cm^2 under a negative bias. The breakdown fields of the reference and the F-O_2 samples are approximately 1.2–1.9 MV/cm and that of the PE-N_2O sample is 2.7 MV/cm. The excellent breakdown field of the ICP-N_2O sample is 4.2 MV/cm. The improvement in breakdown field is attributed to the reduced surface roughness after treatments. A smooth surface can suppress the local accumulation of electrons and is responsible for the uniform electric field, and hence the ICP-N_2O sample has a high breakdown field.

Figure 4 depicts the proposed schematic diagram of N_2O plasma treatment on the Ta_2O_5 film based on the above results. Plasma treatment modifies the surface and causes ion bombardment effects. The principal dissociation products (N, O, and NO) of N_2O would modify the surface of Ta_2O_5 films. The O atoms were accelerated

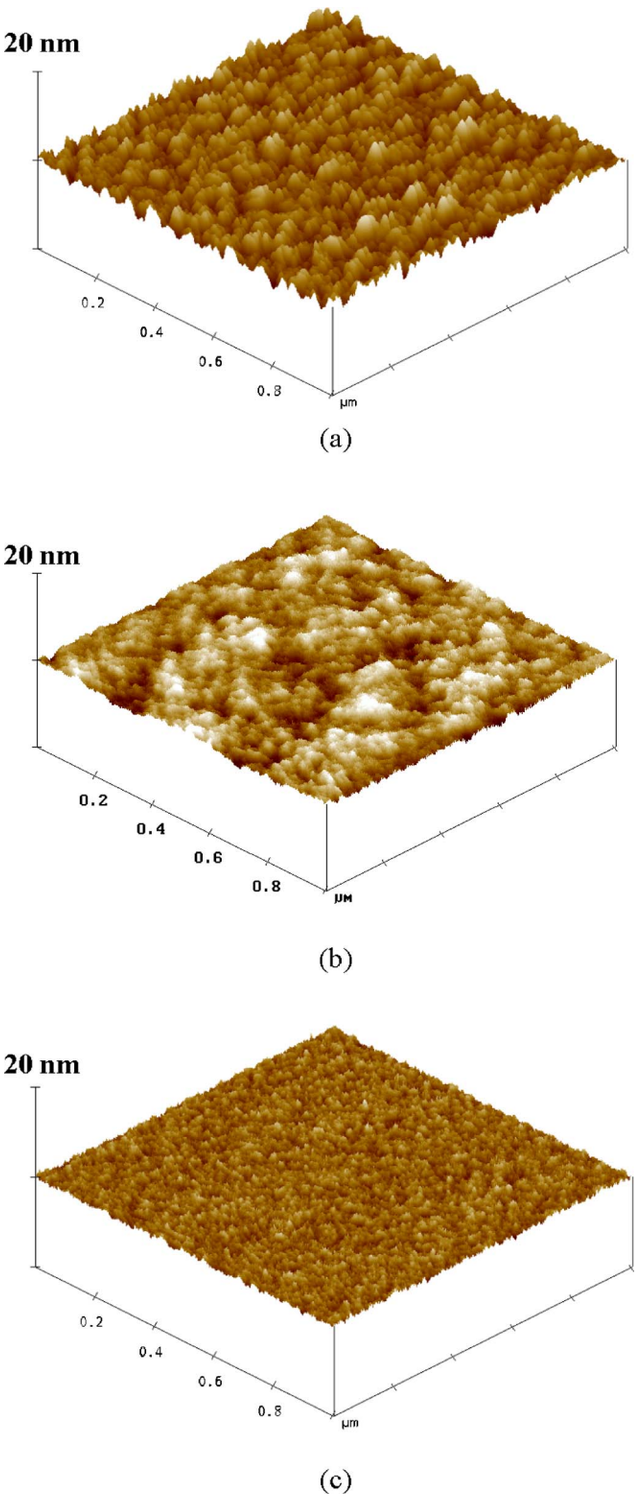

Figure 3. (Color online) AFM images of Ta_2O_5 surfaces after (a) furnace annealing at 400°C for 30 min, (b) PE treatment at 250°C for 5 min, and (c) ICP treatment at 250°C for 5 min.

toward the Ta_2O_5 film, where they were adsorbed and incorporated in oxygen vacancies. The dissociation of gas importantly affects the results of plasma treatment. The leakage current density of the ICP-N_2O sample is 1 order of magnitude lower than that of the PE-N_2O sample at an electric field of −1 MV/cm, because the concentration of oxygen vacancy is lower and the effect of nitridation is higher following ICP than PE treatment.

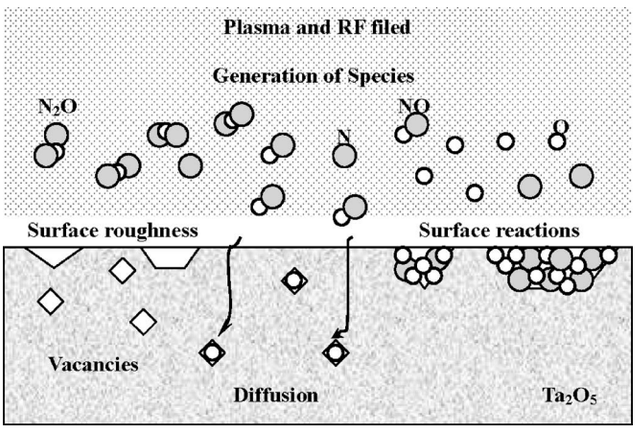

Figure 4. Schematic illustration for N_2O plasma treatment on the Ta_2O_5 film.

Figure 5 shows the leakage current density vs time characteristics at high stress electric fields. More than ten capacitors were measured for each post-treatment and one typical curve is shown in the study. At the beginning of the stress test, the leakage current fell rapidly. The decrease in the leakage current was believed to be caused by electron trapping.[22,23] The drop was gradual during the middle stage of the stress test. However, the leakage current rapidly increased and fatal breakdown occurred after the stress was applied for a longer period. Fatal breakdown is defined as the leakage current density increases to 10^{-3} A/cm^2 or ten times higher than the value at the previous 1 s time step. The data indicates that lower leakage films have longer breakdown lifetime. The ICP-N_2O sample has a lower leakage current and longer breakdown lifetime under the stress at a constant electric field of 1.8 MV/cm. The leakage currents in F-O_2 and PE-N_2O samples are higher and associated with a shorter time to breakdown at constant fields of 1.2 and 1.6 MV/cm, respectively. Breakdown is manifested by the formation of a conductive path through the oxide initiated by the presence of weak spots.[24] Local field enhancements at the weak spots cause vacancy-related breakdown. The high-density local vacancies, including

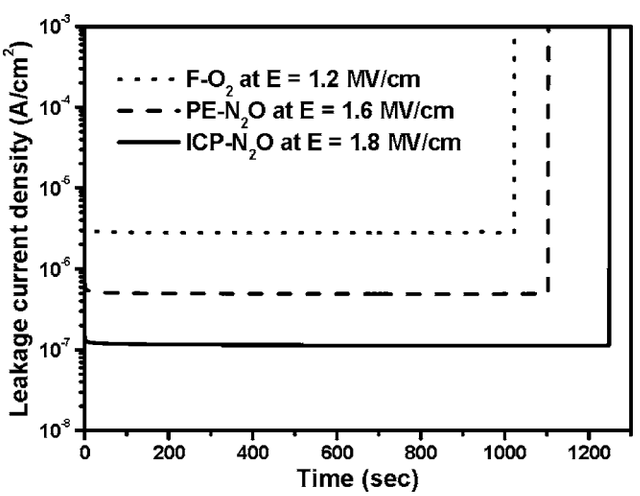

Figure 5. Leakage current density vs time plots for F-O_2 sample under 1.2 MV/cm, PE-N_2O sample under 1.6 MV/cm, and ICP-N_2O sample under 1.8 MV/cm.

Table I. Properties of $Ta/Ta_2O_5/Ta$ capacitors with various post-treatments.

	Reference	F-O_2	PE-N_2O	ICP-N_2O
Roughness (nm)	1.53	1.35	0.75	0.45
Leakage current (A/cm^2) at $E = 1$ MV/cm	4.5×10^{-7}	2.4×10^{-7}	2.7×10^{-8}	2.1×10^{-8}
Leakage current (A/cm^2) at $E = -1$ MV/cm	3.8×10^{-7}	5.7×10^{-8}	3.8×10^{-9}	4.0×10^{-10}
Breakdown field (MV/cm) at 10^{-6} A/cm^2under a negative bias	1.2	1.9	2.7	4.2
Breakdown field (MV/cm) at 10^{-6} A/cm^2 under a positive bias	1.2	1.9	3	3.4
Dielectric constant	~19	20–23	19–21	19–21
Electric field of 10 year lifetime (MV/cm)		0.87	1.23	1.61

traps, are responsible for vacancy-related breakdown. Furthermore, TDDB lifetime was studied under various equivalent electric fields. The ICP-N_2O sample exhibits a longer term reliability than the PE-N_2O, F-O_2, and reference samples and the samples in Ref. 12. The extrapolated long-term lifetime demonstrates that the ICP-N_2O sample can survive 10 years at a stress field of 1.61 MV/cm, as listed in Table I.

The leakage current in the $Ta/Ta_2O_5/Ta$ capacitor may be due to several mechanisms, including Schottky emission, Poole–Frenkel effect, electronic hopping conduction, and tunneling.[4,6,24,25] The *J-E* characteristics of MIM capacitors are highly asymmetric with the voltage polarity for the Schottky emission. In this study, asymmetric *J-E* characteristics were observed, as shown in Fig. 1. The Schottky current is due to electrons which transit above the potential barrier at the surface of a metal or semiconductor and is typical of the electrode-limited current. A *J-E* relation for Schottky emission is given by the following equation[4,6,25]

$$J = AT^2 \exp\left(-\frac{q\phi_0}{kT}\right)\exp\left(\frac{\beta}{kT}E^{1/2}\right) \quad [5]$$

where J is the current density, A is a constant, T denotes the absolute temperature, q is the electronic charge, ϕ_0 is the barrier height, k represents the Boltzmann constant, E represents the electric field, and β is defined as

$$\beta = \left(\frac{q^3}{4\pi\varepsilon_0\varepsilon}\right)^{1/2} \quad [6]$$

where ε_0 is the permittivity of free space and ε represents the high-frequency dielectric constant. Figure 6 shows the logarithmic current density as a function of the square root of the electric field [$\log(J)$ vs $E^{1/2}$]. A good linearity is observed for the plots, indicating that the Schottky emission is the possible dominant conduction mechanism for leakage currents, whereby electrons from the cathode overcome the Ta/Ta_2O_5 energy barrier before being emitted into the Ta_2O_5. The Schottky emission can be explained as follows. When an electron enters the dielectric, it produces an image field that adds and lowers the barrier field, resulting in a reduced barrier height and an enhanced current given.

Figure 7 illustrates the conduction mechanism of the $Ta/Ta_2O_5/Ta$ capacitor in the study. The Schottky emission is the possible dominant conduction mechanism for leakage currents. Surface roughness and oxygen vacancy are attributed to the resulting conduction mechanism. The F-O_2 sample has a rougher surface than the ICP-N_2O sample, as shown in Fig. 3. It was reported that surface roughness yields on the image potential were as high as even 10–60% compared to that of a flat interface.[21] Some activated oxygen in the Ta_2O_5 film could escape or diffuse into and react with the Ta bottom electrode layer during furnace annealing. The oxygen vacancy acts as an electron trap with certain trap level in the energy band diagram. The traps act as stepping sites for electrons and facilitate their transport through the oxide. Moreover, the barrier height becomes low when the oxygen vacancies accumulate at the interface of the Ta_2O_5–metal electrode.[6,26] ICP treatments cause more surface modification and less oxygen diffusion compared to furnace annealing treatments. The F-O_2 sample has a higher interfacial barrier compared to the ICP-N_2O sample due to higher surface roughness and oxygen vacancy concentration. When the top electrode is negatively biased, electrons are relatively easily injected from the Ta top electrode into the tantalum oxide layer and further conductivity is governed via trap sites.

Conclusions

The electrical properties of Ta_2O_5 thin films with MIM structures following the ICP-N_2O post-treatments were examined. The result-

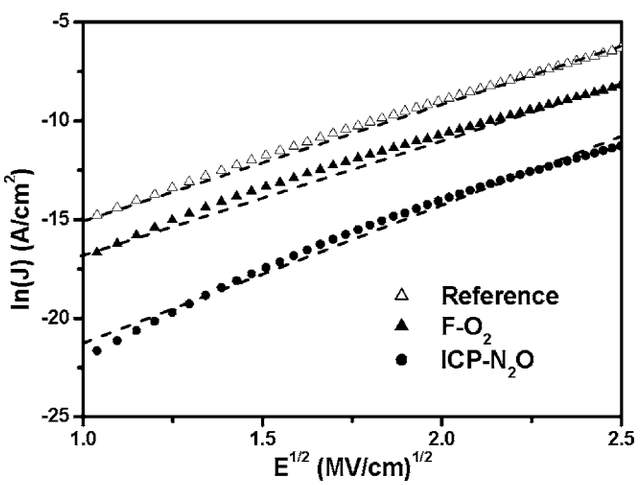

Figure 6. The $\ln(J)$ vs $E^{1/2}$ plots for various $Ta/Ta_2O_5/Ta$ capacitors.

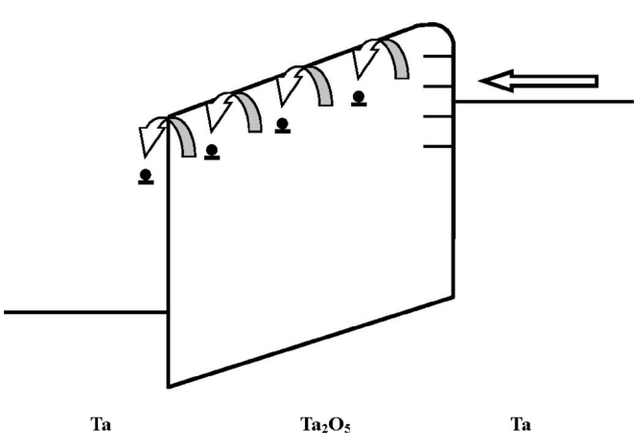

Figure 7. Schematic illustration of the conduction mechanism in the $Ta/Ta_2O_5/Ta$ capacitor.

ing $Ta/Ta_2O_5/Ta$ capacitors have low leakage current densities (4.0×10^{-10} A/cm^2 under 1 MV/cm), high breakdown fields (4.2 MV/cm at 10^{-6} A/cm^2), and lifetimes of over 10 years at 1.61 MV/cm due to effectively dissociated N_2O gas. The leakage current of the $Ta/Ta_2O_5/Ta$ capacitor is dominated by Schottky emission. Oxygen vacancy and surface roughness are attributed to the resulting conduction mechanism in the study. The low-temperature ICP treatment reduces the diffusion of oxygen atoms into the Ta bottom electrode and lessens the oxygen vacancies, while the reactions of energetic radicals and ions reduce surface roughness. Consequently, the electrical characteristics and reliability of $Ta/Ta_2O_5/Ta$ capacitors are enhanced after the low-temperature ICP treatments.

Acknowledgment

This work was financially supported by the National Science Council of the Republic of China under contract no. NSC 94-2215-E-492-009 and, in part, by the Ministry of Economic Affairs of the Republic of China under contract no. 95-EC-17-A-08-S1-0003.

National Nano Device Laboratories assisted in meeting the publication costs of this article.

References

1. T. P. Liu, W. P. Huang, and T. B. Wu, *IEEE Trans. Electron Devices*, **50**, 1425 (2003).
2. J. W. Kim, S. D. Nam, S. H. Lee, S. J. Won, W. D. Kim, C. Y. Yoo, Y. W. Park, S. I. Lee, and M. Y. Lee, in *Tech. Dig. - Int. Electron Devices Meet.*, **1999**, 793.
3. J. Y. Tewg, Y. Kuo, J. Lu, and B. W. Schueler, *J. Electrochem. Soc.*, **151**, F59 (2004).
4. C. Chaneliere, J. L. Autran, R. A. B. Devine, and B. Balland, *Mater. Sci. Eng., R.*, **22**, 269 (1998).
5. W. F. Wu, K. L. Ou, C. P. Chou, and C. C. Wu, *J. Electrochem. Soc.*, **150**, G83 (2003).
6. K. C. Tsai, W. F. Wu, C. G. Chao, and C. P. Kuan, *J. Electrochem. Soc.*, **153**, G492 (2006).
7. T. Aoyama, S. Saida, Y. Okayama, M. Fujisaki, K. Imai, and T. Arikado, *J. Electrochem. Soc.*, **143**, 977 (1996).
8. W. R. Hitchens, W. C. Krusell, and D. M. Dobkin, *J. Electrochem. Soc.*, **140**, 2615 (1993).
9. J. M. Shieh, K. C. Tsai, and B. T. Dai, *Appl. Phys. Lett.*, **81**, 1294 (2002).
10. K. C. Tsai, J. M. Shieh, and B. T. Dai, *Electrochem. Solid-State Lett.*, **6**, F31 (2003).
11. S. V. Nguyen, *IBM J. Res. Dev.*, **43**, 109 (1999).
12. S. Ezhilvalavan and T. Y. Tseng, in *Proceedings of the Electronic Components and Technology Conference*, p. 1042 (1999).
13. S. C. Sun and T. F. Chen, *IEEE Electron Device Lett.*, **EDL-17**, 355 (1996).
14. K. C. Tsai, W. F. Wu, J. C. Chen, C. G. Chao, and T. J. Pan, *J. Electrochem. Soc.*, **152**, G83 (2005).
15. K. C. Tsai, W. F. Wu, J. C. Chen, C. G. Chao, and T. J. Pan, *J. Vac. Sci. Technol. B*, **22**(3), 993 (2004).
16. W. S. Lau, M. T. C. Perera, P. Babu, A. K. Ow, T. Han, N. P. Sandler, C. H. Tung, T. T. Sheng, and P. K. Chu, *Jpn. J. Appl. Phys., Part 2*, **37**, L435 (1998).
17. B. C. Smith, A. Khandelwal, and H. H. Lamb, *J. Vac. Sci. Technol. B*, **18**, 1757 (2000).
18. Y. Vota, J. Hander, and A. A. Saleh, *J. Vac. Sci. Technol. A*, **18**, 372 (2000).
19. D. W. Hess, *IBM J. Res. Dev.*, **43**, 127 (1999).
20. S. Blonkowski, M. Regache, and A. Halimaoui, *J. Appl. Phys.*, **90**, 1501 (2001).
21. Y. S. Kim, Y. H. Lee, K. M. Lim, and M. Y. Sung, *Appl. Phys. Lett.*, **74**, 2800 (1999).
22. C. Chen, S. E. Holland, and C. Hu, *IEEE Trans. Electron Devices*, **ED-32**, 413 (1985).
23. S. Yamamichi, A. Yamamichi, D. Park, T. J. King, and C. Hu, *IEEE Trans. Electron Devices*, **46**, 342 (1999).
24. E. Atanassova, N. Novkovski, A. Paskaleva, and M.-P. Gjorgjevich, *Solid-State Electron.*, **46**, 1887 (2002).
25. S. M. Sze, *Physics of Semiconductor Device*, p. 402, Wiley, New York (1981).
26. J. H. Joo, Y. C. Jeon, J. M. Seon, K. Y. Oh, J. S. Roh, and J. J. Kim, *Jpn. J. Appl. Phys., Part 1*, **36**, 4382 (1997).